


Depinning in the quenched Kardar-Parisi-Zhang class. II. Field theory

Gauthier Mukerjee and Kay Jörg Wiese 

Laboratoire de Physique de l'École Normale Supérieure, ENS, Université PSL, CNRS, Sorbonne Université, Université Paris-Diderot, Sorbonne Paris Cité, 24 rue Lhomond, 75005 Paris, France



(Received 28 July 2022; accepted 20 April 2023; published 30 May 2023)

There are two main universality classes for depinning of elastic interfaces in disordered media: quenched Edwards-Wilkinson (qEW) and quenched Kardar-Parisi-Zhang (qKPZ). The first class is relevant as long as the elastic force between two neighboring sites on the interface is purely harmonic and invariant under tilting. The second class applies when the elasticity is nonlinear or the surface grows preferentially in its normal direction. It encompasses fluid imbibition, the Tang-Leschorn cellular automaton of 1992 (TL92), depinning with anharmonic elasticity (aDep), and qKPZ. While the field theory is well developed for qEW, there is no consistent theory for qKPZ. The aim of this paper is to construct this field theory within the functional renormalization group (FRG) framework, based on large-scale numerical simulations in dimensions $d = 1, 2$, and 3 , presented in a companion paper [Mukerjee *et al.*, *Phys. Rev. E* **107**, 054136 (2023)]. In order to measure the effective force correlator and coupling constants, the driving force is derived from a confining potential with curvature m^2 . We show, that contrary to common belief, this is allowed in the presence of a KPZ term. The ensuing field theory becomes massive and can no longer be Cole-Hopf transformed. In exchange, it possesses an IR attractive stable fixed point at a finite KPZ nonlinearity λ . Since there is neither elasticity nor a KPZ term in dimension $d = 0$, qEW and qKPZ merge there. As a result, the two universality classes are distinguished by terms linear in d . This allows us to build a consistent field theory in dimension $d = 1$, which loses some of its predictive powers in higher dimensions.

DOI: [10.1103/PhysRevE.107.054137](https://doi.org/10.1103/PhysRevE.107.054137)

I. INTRODUCTION

Disordered elastic manifolds exhibit universal critical behavior when driven slowly, known as *depinning*. There are two main universality classes, each associated with a stochastic differential equation of evolution: quenched Edwards-Wilkinson (qEW) [1] and quenched Kardar-Parisi-Zhang (qKPZ) [2]. The first class is relevant as long as the elasticity of the interface is purely harmonic and invariant under tilting. This description is valid in a variety of situations such as magnetic domain walls in the presence of disorder a.k.a. the Barkhausen effect [3–6], vortex lattices [7,8], charge-density waves [9], and DNA unzipping [10]. While these systems have short-ranged elasticity, this framework can readily be adapted to describe systems with long-range (LR) elasticity such as contact-line depinning [11–13], earthquakes [14,15], and knitting [16,17].

The second class is relevant when the elasticity is nonlinear or the surface grows preferentially in its normal direction. It encompasses fluid imbibition [18], the Tang-Leschorn cellular automaton of 1992 (TL92) [19] or its variants [20], depinning with anharmonic elasticity (aDep) [21], and qKPZ [2]. That all these models are in the same universality class is nontrivial but is now firmly established [22]. This so-called qKPZ class has been observed for magnetic domain walls [23,24], in growing bacterial colonies [25], and chemical reaction fronts [26].

While the field theory for qEW is well established [1,27–33], building a field theory for qKPZ is a challenge. It has previously been attempted in Ref. [34]. In that work, the running coupling constant for the nonlinearity goes to infinity.

The first question one needed to clarify was whether this is true or an artifact of the functional renormalization group (FRG) treatment. In Ref. [22] we measured in a numerical simulation the effective action of three models: qKPZ, TL92, and aDep. For $d = 1$ we found that all three possess an effective long-distance behavior fully described by the terms in the qKPZ equation,

$$\eta \partial_t u(x, t) = c \nabla^2 u(x, t) + \lambda [\nabla u(x, t)]^2 + m^2 [w - u(x, t)] + F(x, u(x, t)). \quad (1)$$

The disorder forces $F(x, u)$ are quenched Gaussian random variables with variance

$$\overline{F(x, u)F(x', u')} = \delta^d(x - x') \Delta_0(u - u'). \quad (2)$$

$\Delta_0(u)$ is the microscopic disorder-force correlator, assumed to decay rapidly for short-range (SR) disorder. In higher dimensions the same conclusions were reached, although with larger uncertainties.

Motivated by these findings, we reconsider the field theory corresponding to Eq. (1). There are two key observations. First of all, for $d \rightarrow 0$, three universality classes merge: qKPZ, qEW with short-ranged, and qEW with LR interactions. This is visualized in Fig. 1. The second key observation is that the way we drive the system is important. In fact, we drive with a force that derives from a confining potential, the term $m^2[w - u(x, t)]$ in Eq. (1). That allows us to measure the

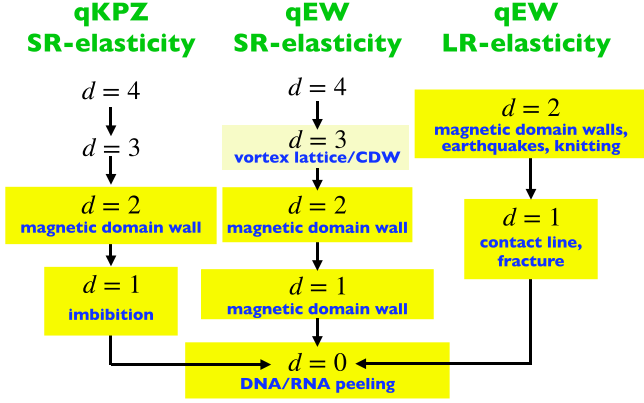


FIG. 1. Universality classes at depinning, for $d < d_c$. For the yellow-shaded cases experiments exist.

effective force correlator $\Delta(w)$ defined via

$$\Delta(w - w') := m^4 L^d \overline{(u_w - w)(u_{w'} - w')}, \quad (3)$$

$$u_w := \frac{1}{L^d} \int_x u_w(x), \quad (4)$$

$$u_w(x) := \lim_{t \rightarrow \infty} u(x, t) \text{ given } w \text{ fixed.} \quad (5)$$

In this protocol, w is increased in steps. One then waits until the interface stops, which defines $u_w(x)$. Its center-of-mass position is u_w , and its fluctuations define $\Delta(w)$.

This driving force appears in the effective action (6) as a mass term, as compared to [34], which considered a massless theory. Their motivation was that a massive term breaks Galilean invariance, and this is something “you do not want for the KPZ equation.” We believe that this is not a problem here, for two reasons: First of all, Galilean invariance is already broken by the quenched disorder $F(x, u)$, even after disorder averaging. Second, even if the driving breaks Galilean invariance, this should affect only large-scale properties but not small-scale ones (small with respect to the correlation length), and especially not critical properties.

There is a price to pay for introducing a massive term: one loses the Cole-Hopf transformation, a transformation that allows one to map the KPZ equation to a simpler stochastic heat equation with multiplicative noise (see Sec. III F). This the authors of Ref. [34] were not ready to give up, as it complicates perturbation theory. As we will see below, it breaks the nonrenormalization of λ/c , allowing us to find a fixed point for the latter. As both the massive and the massless scheme give, at least in one-loop order, the same results close to the upper critical dimension $d_c = 4$, what we will present below is not a systematic ε -expansion. Rather, if we suppose we know the FRG fixed point for qEW, then our scheme allows us to control qKPZ perturbatively in d , in an expansion around the qEW fixed point. While the latter is known analytically in $d = 0$ [35], what we use here is the one-loop fixed point, obtained via the $\varepsilon = 4 - d$ expansion. The latter is actually quite good even down to $d = 1$: It predicts a roughness exponent of $\zeta = 1$, as compared to the best numerical value of $\zeta = 5/4$ [36,37]. The FRG correlator is, even quantitatively, rather well approximated by its one-loop value [1,6]. We

restrict ourselves here to one-loop order, which has the benefit of greater transparency. Preliminary calculations show that extension to two-loop order is straightforward though cumbersome. The method we present below allows us to compute analytically the different critical exponents as well as the full force correlator and present quantitative agreement with the numerical simulations.

This paper is organized as follows: In the next Sec. II we first define the field theory and review perturbation theory (Sec. II A). We then summarize scaling arguments described in detail in the companion paper [22] (Sec. II B). The effective force correlator is defined in Sec. II C, and the relation to directed percolation in Sec. II D, followed by a discussion of the effective action measured in simulations (Sec. II E). Section III is dedicated to the field theory. We start with a review of the generation of the KPZ term from an anharmonic elasticity (Sec. III A). All one-loop contributions are given in Sec. III B, with details relegated to the Appendix. Section III C establishes the flow equations. Necessary conditions for their solution are derived in Sec. III D, followed by an analytical solution in Sec. III E, first giving the scheme (Sec. III E 1) and then explicit values in $d = 1$ to $d = 3$ (Secs. III E 2–III E 4). Tables summarize our findings in Sec. III E 6. We comment on the Cole-Hopf transformation (Sec. III F) and present in layman’s terms physical insights from our work (Sec. IV), before concluding in Sec. V.

II. MODEL AND PHENOMENOLOGY

A. Model, action, and perturbation theory

The Martin-Siggia-Rose [38] action corresponding to Eq. (1) reads

$$\begin{aligned} \mathcal{S}[u, \tilde{u}] = & \int_{x,t} \tilde{u}(x, t) \{ \eta \partial_t u(x, t) - c \nabla^2 u(x, t) \\ & - \lambda [\nabla u(x, t)]^2 + m^2 [u(x, t) - w] \} \\ & - \frac{1}{2} \int_{x,t,t'} \tilde{u}(x, t) \Delta_0(u(x, t) - u(x, t')) \tilde{u}(x, t'). \end{aligned} \quad (6)$$

The field $\tilde{u}(x, t)$ is an auxiliary field introduced to enforce Eq. (1) and called the response field. The last term is obtained by averaging $e^{\int_{x,t} \tilde{u}(x, t) F(x, u(x, t))}$ over $F(x, u)$, using its variance (2). Perturbation theory is constructed by expanding around the free theory obtained by setting $\lambda \rightarrow 0$ and $\Delta_0(u) \rightarrow 0$ in Eq. (6). The free response function is the response of the field $u(x + x', t + t')$ to an additional force acting at x', t' ,

$$\begin{aligned} R(x, t) &:= \left\langle \frac{\delta u(x + x', t + t')}{\delta f(x', t')} \right\rangle \\ &= \langle \delta u(x + x', t + t') \tilde{u}(x', t') \rangle. \end{aligned} \quad (7)$$

In Fourier space it reads

$$\begin{aligned} R(k, t) &= \langle \tilde{u}(k, t) u(-k, t') \rangle \\ &= \theta(t' > t) \frac{1}{\eta} e^{-(ck^2 + m^2)(t' - t)/\eta} \\ &= \bullet \longrightarrow \bullet. \end{aligned} \quad (8)$$

Graphically this is represented by an arrow from \tilde{u} to u . The (microscopic) disorder is represented by two dots connected

by a dashed line, whereas the KPZ vertex is a dot with two incoming lines with bars for the derivatives, and one outgoing one. Examples for diagrams correcting the disorder are given in Fig. 3. For an introduction into functional perturbation theory we refer to Sec. 3 of [1]. Note that the disorder is corrected by the KPZ force, and what we loosely call the *renormalized disorder* is more precisely the *renormalized force correlator*, which contains contributions from the KPZ term (see Sec. II C for a detailed discussion). Nontrivial correlations necessitate at least one “disorder” vertex $\Delta_0(u)$. As an example, the leading order to the equal-time two-point function is

$$\begin{aligned} \langle u(k, 0)u(-k, 0) \rangle &= \text{diagram} \\ &= \left[\int_t R(k, t) \right]^2 \Delta_0(0) \\ &= \frac{\Delta_0(0)}{(ck^2 + m^2)^2}. \end{aligned} \quad (9)$$

The arrows represent the response function R , the dotted line the effective force correlator $\Delta_0(u)$. We assume an upper critical dimension of $d_c = 4$ as in qEW. Simulations show that in $d = 3$ the interface is still rough [22], so the upper critical dimension is above 3. Noting that physical realizations can only be constructed in integer dimensions, the remaining open question is whether the four-dimensional system is at its upper critical dimension or potentially above; see Sec. III E 4. Note that an interface in anharmonic depinning is less rough than in qEW; this excludes an upper critical dimension larger than four.

B. Scaling and anomalous exponents

Scaling arguments were given in the companion paper [22]. We recall the main results here. The static two-point function is defined as

$$\frac{1}{2} \overline{[u(x) - u(y)]^2} \simeq \begin{cases} A|x - y|^{2\zeta}, & |x - y| \ll \xi_m, \\ Bm^{-2\zeta_m}, & |x - y| \gg \xi_m. \end{cases} \quad (10)$$

The average is taken over different disorder configurations (there are no thermal fluctuations). ζ is the standard roughness exponent. In contrast to qEW, there is an exponent $\zeta_m > \zeta$. The reason is that the elasticity c renormalizes and thus its anomalous dimension gives rise to another exponent. The quantity ξ_m in Eq. (10) is the correlation length created by the confining potential. Every length parallel to the interface scales as x or ξ_m , whereas in the perpendicular direction it scales as $u \sim x^\zeta \sim \xi_m^\zeta$. To estimate ξ_m , we take $x = \xi_m$ in Eq. (10), obtaining $\xi_m^{2\zeta} \sim m^{-2\zeta_m}$. As a consequence

$$\xi_m \sim m^{-\frac{\zeta_m}{\zeta}}. \quad (11)$$

Note that $\xi_m \not\sim \frac{1}{m}$ as for qEW. Figure 2 shows a scaling collapse of the two-point function with these scalings.

Define ψ_λ , ψ_c , and ψ_η to be the anomalous dimensions of λ , c , and η in units of m^{-1} ,

$$\psi_c := -m\partial_m \ln(c), \quad (12)$$

$$\psi_\lambda := -m\partial_m \ln(\lambda), \quad (13)$$

$$\psi_\eta := -m\partial_m \ln(\eta). \quad (14)$$

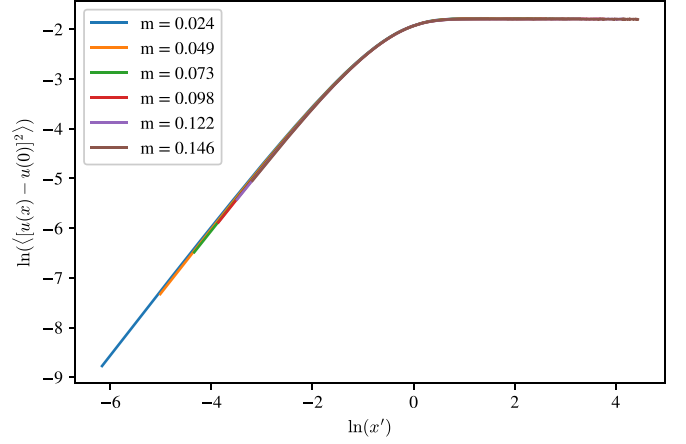


FIG. 2. Scaling collapse of the two-point function (10) obtained by rescaling x and $y = \langle [u(x) - u(0)]^2 \rangle$ such that $x' = \frac{x}{\xi_m} = xm^{\frac{\zeta_m}{\zeta}}$ and $y' = ym^{2\zeta_m}$, in logarithmic scale, for TL92 in $d = 1$.

In order to relate them to the standard scaling exponents ζ , ζ_m , and z , we first need to define z . It is given by the temporal spread of the perturbation in the surface in the two-point function as

$$\frac{1}{2} \overline{[u(x, t) - u(x, t')]^2} \sim |t - t'|^{2\zeta/z}. \quad (15)$$

With these definitions at the fixed point we can derive

$$\frac{\zeta_m}{\zeta} = 1 + \frac{\psi_c}{2}, \quad (16)$$

$$\zeta_m = \psi_c - \psi_\lambda, \quad (17)$$

$$z = \frac{\zeta}{\zeta_m} (2 + \psi_\eta). \quad (18)$$

The first relation is obtained from $x^{-1} \sim q \sim m/\sqrt{c} \sim m^{1+\psi_c/2}$, implying $x^{2\zeta} \sim m^{-(2+\psi_c)\zeta} \equiv m^{-2\zeta_m}$. The second follows from $\lambda u \sim c$. The last one is obtained from $\eta/t \sim m^2$, implying $t \sim m^{-2-\psi_\eta} \sim x^{(2+\psi_\eta)\zeta/\zeta_m}$.

C. The renormalized correlator $\Delta(w)$

In Eq. (3) we had defined the renormalized (effective) force correlator as

$$\Delta(w - w') := m^4 L^d \overline{(u_w - w)(u_{w'} - w')^c}. \quad (19)$$

The definition of u_w is given in Eq. (4). This is the same definition as the one used for qEW [39–42]. Integrating the equation of motion (1) over space for a configuration $u_w(x) := u(x, t)$ at rest yields

$$m^2(w - u_w) + \frac{1}{L^d} \int_x \underbrace{\lambda [\nabla u_w(x)]^2 + F(x, u_w(x))}_{\text{total force}} = 0. \quad (20)$$

Thus the correlator in Eq. (19) measures fluctuations of the *total force*. Only for qEW ($\lambda = 0$) does this equal the force exerted by the disorder. To be specific, let us define

$$F_w := \frac{1}{L^d} \int_x F(x, u_w(x)), \quad (21)$$

$$\Lambda_w := \frac{1}{L^d} \int_x \lambda [\nabla u_w(x)]^2. \quad (22)$$

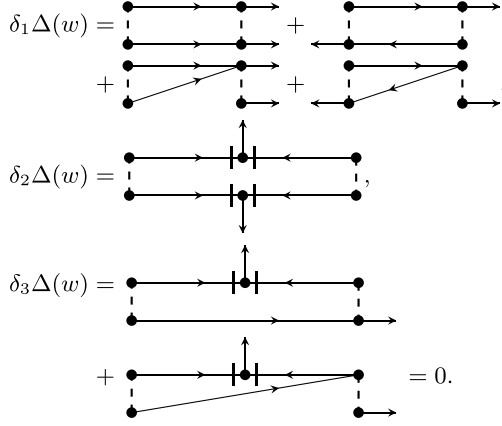


FIG. 3. The three one-loop corrections to $\Delta(w)$ (without combinatorial factors). The dashed line is $\Delta(w)$, the bars are the spatial derivatives of the KPZ term; notations as in [33]. The first one $\delta_1 \Delta(w)$ contains the qEW terms. The second contribution $\delta_2 \Delta(w) \sim \lambda^2 \Delta(w)^2$ is an additional term, present in qKPZ but not in qEW. The next two terms $\delta_3 \Delta(w) \sim \lambda \Delta(w) \Delta'(w)$ cancel each other; they also vanish separately since they are odd in w , whereas $\Delta(w)$ is even.

A configuration at rest then has

$$m^2(w - u_w) + F_w + \Lambda_w = 0. \quad (23)$$

Our goal is to compare observables with objects in the field theory. What is calculated there is the effective action, or more precisely its two-time contribution. (In the statics this would be the two-replica term.) It is the sum of all connected two-time diagrams, i.e., with two external \tilde{u} fields. To one-loop order, these are shown in Fig. 3. The two-point function \overline{uu}^c is obtained to all orders by contracting the two-time contribution to the effective action with two response functions. While in real space this is a convolution, in momentum and frequency space this is simply a multiplication with the response function $R(k, \omega)$. According to Eq. (19) it is to be evaluated at momentum $k = 0$ and frequency $\omega = 0$. Recall that the response function $R(x, t)$ is the response of the observable $u(x, t)$ to a small uniform kick in force f at $(x, t) = (0, 0)$. Since the center of mass follows the center of the driving parabola w ,

$$f_c = \overline{w - u_w} = \text{const} \Rightarrow \partial_w \overline{u_w} = 1. \quad (24)$$

Thus a uniform kick $f = m^2 \delta w$ leads to a response for the center of mass according to $u_w \rightarrow u_w + \delta w = u_w + \frac{f}{m^2}$. As a result, the integrated response function is given by

$$\int_t R(k = 0, t) \equiv \frac{1}{L^d} \int_x \int_t R(x, t) = \frac{1}{m^2}. \quad (25)$$

This is equivalent to $R(k = 0, \omega = 0) = m^{-2}$.

We finally need to remember the field-theoretic definition of the effective action Γ : It is obtained from the corresponding expectation values by *amputation* of the response function, which is equivalent to dividing by the response function (in Fourier representation). Due to Eq. (25) this is nothing but multiplication with m^2 , once for each of the two external fields u . This gives the factor of m^4 in Eq. (19), and Eq. (19) is nothing but the two-time contribution to the effective action Γ , equivalent to the renormalized force correlator $\Delta(w)$. It is

TABLE I. Numerical values for all exponents used in this section ($d = 1$), as obtained from Ref. [49] combined with the scaling relations derived here.

$\nu_{\parallel} = 1.733847(6)$	$\nu_{\perp} = 1.096854(4)$
$\zeta = 0.632613(3)$	$\zeta_m = 1.046190(4)$
$\frac{\zeta_m}{\zeta} = 1.65376(1)$	$\tau = 1.259246(3)$
$\beta_{\text{dep}} = 0.636993(7)$	$\psi_{\lambda} = 0.26133(2)$
$\psi_k = 1.30752(2)$	

the ($k = 0, \omega = 0$) mode of the full effective force correlator in the field theory for depinning.

Having established that Eq. (19) is the proper definition of the renormalized $\Delta(w)$, it is still instructive to study the correlations of all three forces appearing in Eq. (20). To this aim, let us define in addition to Eq. (19)

$$\Delta_{FF}(w - w') := L^d \overline{F_w F_{w'}^c}, \quad (26)$$

$$\Delta_{F\Lambda}(w - w') := L^d \overline{F_w \Lambda_{w'}^c}, \quad (27)$$

$$\Delta_{\Lambda\Lambda}(w - w') := L^d \overline{\Lambda_w \Lambda_{w'}^c}. \quad (28)$$

A measurement of these quantities is shown below in Fig. 11.

Let us finally give the scaling dimensions,

$$\Delta(0) \sim m^4 \xi_m^d (u_w - w)^2 \sim m^{4-d\frac{\zeta_m}{\zeta}-2\zeta_m}. \quad (29)$$

The scaling of the argument of $\Delta(w)$ is given by

$$w \simeq u \sim m^{-\zeta_m}. \quad (30)$$

These scalings are reflected in the FRG flow equations derived below in Eq. (55).

D. Link to directed percolation, exponents given in the literature, and other relations

For TL92 in $d = 1$, the scaling of a blocked interface at depinning is given by directed percolation [19,20,43–46]. In Table I we summarize the exponents obtained this way, which guide us in the construction and tests of the FRG. Details are given in [22].

In dimensions $d \geq 2$ directed percolation paths are one-dimensional, whereas the interface is d -dimensional. As a result, the mapping to DP no longer exists, and one has to introduce directed surfaces [43]. The exponents we find in $d = 2$ and $d = 3$ are summarized in Table III below.

E. The effective action in simulations

To guide our field-theoretical work, we first checked in dimension $d = 1$ that the scaling exponents given in Table I account for the measured values of ψ_c and ψ_{λ} given in Eqs. (12) and (13). To this aim, an algorithm was designed [22] to measure ψ_c and ψ_{λ} by imposing a spatial modulation in the background-field configuration w . The simulations were performed for three different models, all in the qKPZ universality class: the cellular automaton TL92 [19], anharmonic depinning [21,22], and a direct simulation of Eq. (1) [22]. The best results were achieved for anharmonic depinning, due to an efficient algorithm for its evolution [21].

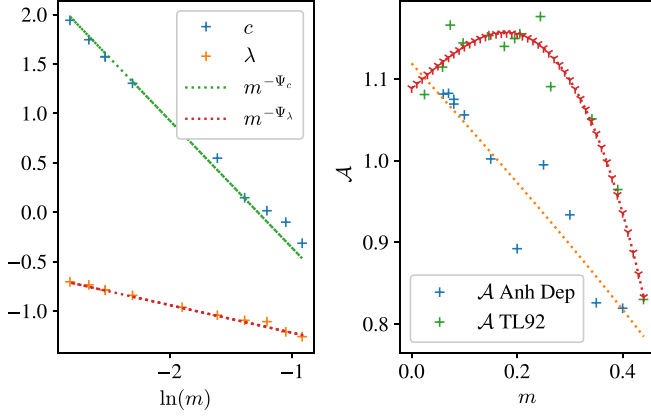


FIG. 4. Left: Effective c and λ for anharmonic depinning. Right: Convergence to the fixed point as $m \rightarrow 0$, for both anharmonic depinning and TL92. The dotted lines are guides for the eye.

With the algorithm designed in [22], we measured the effective couplings λ and c , as a function of m . In Fig. 4 (left) we show their flow as a function of m . To be specific, what we measure (left), and what is predicted from DP via Table I (right) is

$$\psi_c^{d=1} = 1.31(4), \quad \psi_c^{\text{DP}} = 1.30752(2), \quad (31)$$

$$\psi_\lambda^{d=1} = 0.28(3), \quad \psi_\lambda^{\text{DP}} = 0.26133(2). \quad (32)$$

This confirms our scaling analysis and allows us to measure as shown in Fig. 4 the dimensionless amplitude

$$\mathcal{A} := \frac{\Delta(0)}{|\Delta'(0^+)|} \frac{\lambda}{c}. \quad (33)$$

The idea behind this definition is that the KPZ term has one field more than the elastic term. Thus the ratio λ/c has the inverse dimension of a field, which is compensated by the first ratio. That \mathcal{A} converges to the same value for two different models gives strong evidence that qKPZ is the effective theory, and that a fixed point of the renormalization-group flow is reached. In $d = 1$, this ratio reads

$$\mathcal{A}^{d=1} = 1.10(2). \quad (34)$$

The last points to verify are that we can measure the effective-force correlator $\Delta(w)$, that different models in the qKPZ class have the same $\Delta(w)$, and that this function is close to, but distinct from, the one for qEW. This is shown in Fig. 12 below.

III. FIELD THEORY

Now that we verified that all models have a fixed point represented by the qKPZ equation, and that we have the correct scaling dimensions for every variable, we can confidently construct their field theory.

A. Reminder: Generation of KPZ term from anharmonic elasticity

Let us recall how anharmonic elastic terms generate a KPZ term at depinning [34]: To this purpose consider a standard

elastic energy, supplemented by an additional anharmonic (quartic) term (setting $c = 1$ for simplicity),

$$\mathcal{H}_{\text{el}}[u] = \int_x \frac{1}{2} [\nabla u(x)]^2 + \frac{c_4}{4} [(\nabla u(x))^2]^2. \quad (35)$$

The corresponding terms in the equation of motion read

$$\partial_t u(x, t) = \nabla^2 u(x, t) + c_4 \nabla \{ \nabla u(x, t) [\nabla u(x, t)]^2 \} + \dots \quad (36)$$

Since the r.h.s. of Eq. (36) is a total derivative, it is surprising that a KPZ term can be generated in the limit of a *vanishing* driving velocity. This puzzle was solved in Ref. [34], where the KPZ term arises by contracting the nonlinearity with one bare disorder (we drop the index on Δ_0 from now on for simplicity of notation),

$$\delta\lambda = -\frac{c_4}{p^2} \int_{t>0} \int_{t'>0} \int_k e^{-(t+t')(k^2+m^2)} [k^2 p^2 + 2(kp)^2] \times \Delta'(u(x, t+t') - u(x, 0)). \quad (37)$$

As $u(x, t+t') - u(x, 0) \geq 0$, the leading term in Eq. (37) can be written as

$$\delta\lambda = -\frac{c_4}{p^2} \int_{t>0} \int_{t'>0} \int_k e^{-(t+t')(k^2+m^2)} [k^2 p^2 + 2(kp)^2] \Delta'(0^+). \quad (38)$$

Integrating over t, t' and using the radial symmetry in k yields

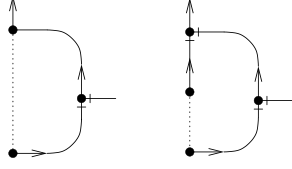
$$\delta\lambda = -c_4 \left(1 + \frac{2}{d}\right) \int_k \frac{\Delta'(0^+) k^2}{(k^2 + m^2)^2}. \quad (39)$$

This shows that in the FRG a KPZ term is generated from the nonlinearity. As $-\Delta'(0^+) > 0$, its amplitude is positive. The integral (39) has a strong UV divergence; thus the generation of this term happens at small scales, similar to the generation of the critical force; see the Appendix A 3.

B. One-loop contributions

Here we summarize the one-loop contributions to c, λ, η , and Δ . This is *almost* the same calculation as in Ref. [34], with a little twist: Since we work in a massive scheme, many of the cancellations in [34] no longer exist. We remind that this change in scheme was forced upon us by our decision to measure the effective parameters of the theory, necessitating our driving with a confining potential. We believe that this is also much closer to real experiments. It is a scheme widely used for perturbative RG for the Ising model in $d = 3$, pioneered by Parisi and used up to seven-loop order by Nickel and collaborators [47–51]. As discussed above, we think of this fixed-dimension renormalization scheme as an expansion around the $d = 0$ qEW fixed point. The diagrams from the perturbation in λ are given in Figs. 5–7.

We obtain the same diagrams as in [34] but with coefficients a_i that differ from [34] away from the upper critical

FIG. 5. The one-loop corrections to c .

dimension. The explicit calculations are given in the Appendix. Terms with numerical coefficients only (no a_i) are those appearing already in qEW:

$$\frac{\delta\eta}{\eta} = -[a_0\hat{\lambda}\Delta'(0^+) + \Delta''(0^+)]I_1, \quad (40)$$

$$\frac{\delta c}{c} = -[a_1\hat{\lambda}\Delta'(0^+) + a_2\hat{\lambda}^2\Delta(0)]I_1, \quad (41)$$

$$\frac{\delta\lambda}{\lambda} = -[a_3\hat{\lambda}\Delta'(0^+) + a_4\hat{\lambda}^2\Delta(0)]I_1, \quad (42)$$

$$\delta\Delta(u) = \left\{ a_5\hat{\lambda}^2\Delta(u)^2 - \partial_u^2 \frac{1}{2} [\Delta(u) - \Delta(0)]^2 \right\} I_1, \quad (43)$$

$$\hat{\lambda} := \frac{\lambda}{c}, \quad (44)$$

$$I_1 = \int_k \frac{1}{(ck^2 + m^2)^2}, \quad (45)$$

$$a_0 = \frac{d}{4}, \quad a_1 = 1, \quad a_2 = \frac{d-1}{3}, \quad (46)$$

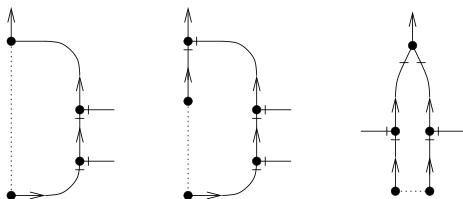
$$a_3 = 1, \quad a_4 = \frac{d+2}{6}, \quad a_5 = \frac{d(d+2)}{12}. \quad (47)$$

The coefficients a_i in the limit of $d \rightarrow 4$ used by [34] are obtained by setting $d \rightarrow 4$, resulting into $a_i = 1$ for all i , except $a_5 = 2$. While this is the standard procedure followed in a dimensional expansion, it misses that in dimension $d = 0$ the KPZ term does not exist, and thus cannot correct the remaining terms: viscosity η , and effective force correlator $\Delta(u)$. The factors of d in coefficients a_0 and a_5 reflect this physical necessity. No such constraint exists for c and λ : since they are absent from the equation of motion (1) in $d = 0$, their coefficients can well be modified.

As λ and c appear in the combination of $\hat{\lambda} = \lambda/c$, the important question is whether this ratio is corrected. This is indeed the case as

$$\frac{\delta\hat{\lambda}}{\hat{\lambda}} = (a_2 - a_4)\hat{\lambda}^2\Delta(0)I_1 = -\frac{4-d}{6}\hat{\lambda}^2\Delta(0)I_1. \quad (48)$$

Note that this term is negative and has a power in $\hat{\lambda}$ superior to one. It will therefore stop the RG flow for $\hat{\lambda}$ at large $\hat{\lambda}$, allowing us to close our system of equations!

FIG. 6. One-loop diagrams correcting λ .FIG. 7. Additional one-loop correction to η for qKPZ as compared to qEW.

A final important point to mention is that the confining potential $\sim m^2$ is not renormalized. In qEW this is due to the statistical tilt symmetry (STS) [1], which can be checked perturbatively: Since the effective force correlator contains u only as a difference $u(x, t) - u(x, t')$, no field u without a time derivative can be generated. The same holds true here: since the additional KPZ vertex has additional spatial derivatives, it cannot generate a field u without spatial derivatives. This property is very useful, as we can as in qEW use m as an RG scale, without caveat.

Finally, the critical force is

$$F_c = F_c^{(1)} + F_c^{(2)} \simeq \left[\Delta'(0^+) + \frac{d}{2}\hat{\lambda}\Delta(0) \right] \int_k \frac{1}{ck^2 + m^2}. \quad (49)$$

The first contribution is negative, identical to qEW. The second is positive, and specific to qKPZ. The nonlinearity reduces the force needed to depin the interface. This is derived in the Appendix A 3.

C. Flow equations

Above we calculated the perturbative corrections. We now derive the corresponding RG relations. Since m is not corrected under renormalization, we use it to parametrize the flow of the remaining quantities. To this aim, first define the dimensionless field as

$$\mathbf{u} := u m^{\zeta_m}. \quad (50)$$

We have $-m \frac{\partial}{\partial m} \Delta(u) = [\delta\Delta]\varepsilon I_1$. The integral I_1 defined in Eq. (45) is evaluated in Eq. (A3) of the Appendix A 1,

$$I_1 := \int_k \frac{1}{(ck^2 + m^2)^2} = \frac{m^{d-4}}{c^{d/2}} \frac{2\Gamma(1 + \frac{\varepsilon}{2})}{\varepsilon(4\pi)^{d/2}}. \quad (51)$$

It scales as

$$I_1 \sim \xi_m^{-d} m^{-4}, \quad (52)$$

where we remind that

$$\Delta(0) \sim \xi_m^d m^4 u^2. \quad (53)$$

The *dimensionless renormalized correlator* $\tilde{\Delta}(\mathbf{u})$ is then defined in terms of the effective force correlator $\Delta(u)$, such that it absorbs εI_1 as

$$\tilde{\Delta}(\mathbf{u}) := \varepsilon I_1 m^{2\zeta_m} \Delta(u = \mathbf{u} m^{-\zeta_m}). \quad (54)$$

The explicit m -dependent factor in front of Δ is the scaling dimension given in Eq. (29). This yields the flow equation for

the effective dimensionless force correlator,

$$\begin{aligned} \partial_t \tilde{\Delta}(u) = & \left(4 - d \frac{\zeta_m}{\zeta} - 2\zeta_m\right) \tilde{\Delta}(u) + u \zeta_m \tilde{\Delta}'(u) \\ & + \frac{d(d+2)}{12} \tilde{\lambda}^2 \tilde{\Delta}(u)^2 \\ & - \tilde{\Delta}'(u)^2 - \tilde{\Delta}''(u) [\tilde{\Delta}(u) - \tilde{\Delta}(0)]. \end{aligned} \quad (55)$$

Here we defined the dimensionless combination $\tilde{\lambda}$

$$\tilde{\lambda} := \frac{\lambda}{c} m^{-\zeta_m} \equiv \hat{\lambda} m^{-\zeta_m}. \quad (56)$$

Its flow equation is obtained from Eq. (48) as

$$-m \partial_m \tilde{\lambda} = \zeta_m \tilde{\lambda} - \frac{4-d}{6} \tilde{\lambda}^3 \tilde{\Delta}(0). \quad (57)$$

It has a fixed point at $\tilde{\lambda} = 0$, and a second nontrivial fixed point at

$$\tilde{\lambda}_c = \sqrt{\frac{6\zeta_m}{(4-d)\tilde{\Delta}(0)}}. \quad (58)$$

We can see that in $d = 4$ the fixed point disappears as $\tilde{\lambda}$ goes to infinity.

The anomalous dimension ψ_c defined in Eq. (12) reads

$$\psi_c = -\tilde{\lambda} \tilde{\Delta}'(0^+) - \frac{d-1}{3} \tilde{\lambda}^2 \tilde{\Delta}(0). \quad (59)$$

Using Eq. (16), we find

$$\frac{\zeta_m}{\zeta} = 1 + \frac{1}{2} \left[-\tilde{\lambda} \tilde{\Delta}'(0^+) - \frac{d-1}{3} \tilde{\lambda}^2 \tilde{\Delta}(0) \right]. \quad (60)$$

Equation (55) is still cumbersome to solve. Reinjecting Eq. (60), we obtain at the fixed point

$$\begin{aligned} 0 = & \left\{ \varepsilon + \frac{d}{2} \left[\tilde{\lambda} \tilde{\Delta}'(0^+) + \frac{d-1}{3} \tilde{\lambda}^2 \tilde{\Delta}(0) \right] - 2\zeta_m \right\} \tilde{\Delta}(u) \\ & + u \zeta_m \tilde{\Delta}'(u) + \frac{d(d+2)}{12} \tilde{\lambda}^2 \tilde{\Delta}(u)^2 \\ & - \tilde{\Delta}'(u)^2 - \tilde{\Delta}''(u) [\tilde{\Delta}(u) - \tilde{\Delta}(0)]. \end{aligned} \quad (61)$$

The anomalous contribution ψ_η reads

$$\psi_\eta = -\left[\frac{d}{4} \tilde{\lambda} \tilde{\Delta}'(0^+) + \tilde{\Delta}''(0^+) \right]. \quad (62)$$

Using Eq. (18) this yields

$$z = \frac{\zeta}{\zeta_m} \left[2 - \frac{d}{4} \tilde{\lambda} \tilde{\Delta}'(0^+) - \tilde{\Delta}''(0^+) \right]. \quad (63)$$

We note that for $d \rightarrow 0$ the contribution of $\tilde{\lambda}$ in Eq. (61) disappears, thus we recover the qEW fixed point. This is not the case in the massless scheme [34]. Increasing d we expect the qKPZ fixed point to smoothly move away from the qEW one. In Fig. 12 below we show that in dimension $d = 1$ the shape of the *measured* $\Delta(w)$ for qEW and qKPZ are close, even though their amplitudes may be rather different. We take this as an encouraging sign to construct the FRG fixed point for qKPZ. This is the task of Sec. III E. Since our expansion is uncontrolled, we need to obtain additional safeguards in order

to see where our approach holds and where it is too crude. For that, we derive constraints to be satisfied by the fixed point.

D. Necessary conditions for a fixed point and bounds

1. Disorder and force correlator relevant

We now assume (as in qEW) that the effective force correlator is relevant, thus $4 - d \frac{\zeta_m}{\zeta} - 2\zeta_m > 0$. This is satisfied in $d = 1$; see Table I. There one finds $4 - d \frac{\zeta_m}{\zeta} - 2\zeta_m = 0.253859$. To compare, in $d = 0$ (qEW) one gets $4 - 2\zeta_m = 4 - 2 \times 2^{-} \approx 0$. In $d = 1$ qEW has $4 - 1 - 2 \times 5/4 = 0.5$.

Taking the limit of $u \rightarrow 0$ in Eq. (61), we obtain a soft bound at one-loop order,

$$|\tilde{\Delta}'(0^+)| > \sqrt{\frac{d(d+2)}{12}} \tilde{\lambda} \tilde{\Delta}(0). \quad (64)$$

When violated, the rescaling term becomes negative, and we expect the effective force correlator to disappear at large scales. Using the definition of the universal amplitude \mathcal{A} in Eq. (33), we can rewrite the bound (64) as¹

$$\mathcal{A} < \mathcal{A}_c^\Delta = \sqrt{\frac{12}{d(d+2)}} = \begin{cases} 2 & \text{in } d = 1 \\ 1.22 & \text{in } d = 2. \\ 0.894 & \text{in } d = 3 \end{cases} \quad (65)$$

2. $\zeta_m > \zeta$

We expect that the effective c would grow at large scales, since it describes the long-distance behavior of models with stronger than harmonic elasticity. As a result we demand that $\psi_c > 0$ (which implies $\zeta_m > \zeta$). Equation (60) then yields

$$\tilde{\lambda} \times \left[\tilde{\Delta}'(0^+) + \frac{d-1}{3} \tilde{\lambda} \tilde{\Delta}(0) \right] < 0. \quad (66)$$

This can be rewritten as

$$\mathcal{A} < \mathcal{A}_c^{\psi_c} = \frac{3}{d-1}. \quad (67)$$

3. Positive pinning force

The last condition is that the critical force at depinning needs to be negative (keeping us pinned), equivalent to a negative square bracket in Eq. (49). In terms of \mathcal{A} , this results in

$$\mathcal{A} \leq \mathcal{A}_c^{f_c} = \frac{2}{d}. \quad (68)$$

We find that in $1 \leq d \leq 4$ the strongest bound is $\mathcal{A}_c^{f_c}$ for the critical force, followed by the one for $\Delta(w)$ and ψ_c ,

$$\mathcal{A} < \mathcal{A}_c^{f_c} \leq \mathcal{A}_c^\Delta < \mathcal{A}_c^{\psi_c}. \quad (69)$$

It would be interesting to continue this to two-loop order.

¹Note that the definition (33) for \mathcal{A} remains unchanged upon replacing all quantities by their dimensionless analog, noted with a tilde.

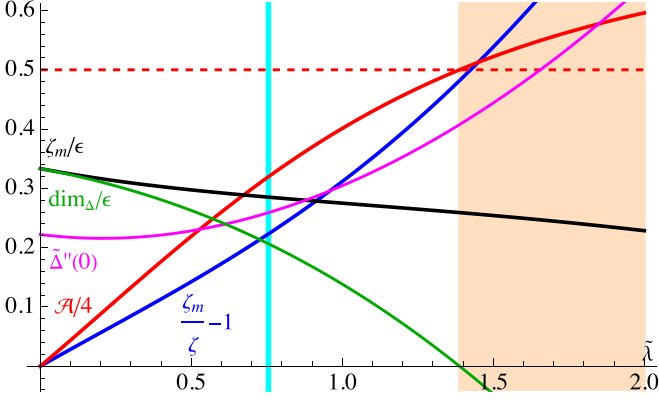


FIG. 8. In $d = 1$: The one-loop contributions ζ_m/ε , amplitude ratio \mathcal{A} and $\zeta_m/\zeta - 1$ as a function of $\tilde{\lambda}$. Setting $d = 1$ in the flow equations. The orange-shaded range is excluded by demanding that Δ is relevant; the cyan line is the location of the fixed point for $\tilde{\lambda}$. The red dashed line is the bound on \mathcal{A} from $\mathcal{A}_c^\Delta = \mathcal{A}_c^{f_c}$. (see Sec. III D 3)

E. Solution of the flow equations

1. Scheme

How do we solve these coupled equations [Eqs. (58)–(63)]? The procedure is adapted from the standard ansatz for qEW [32], explained in detail in Ref. [1]:

- (i) Use the normalization $\tilde{\Delta}(0) = \varepsilon$. In practice, this corresponds to setting $\varepsilon \rightarrow 1$ and $\zeta_m \rightarrow \zeta_m/\varepsilon$ in Eq. (61), and then solving the flow equations with $\tilde{\Delta}(0) \rightarrow 1$ in the code.
- (ii) Solve the (such rescaled) flow equation (61) for $0 \leq \tilde{\lambda} \leq 2$. The correct solution is the one for which $\tilde{\Delta}(w)$ decays to zero at least exponentially fast: A power-law decay, or an increase with w , is not permitted by the physical initial condition.
- (iii) The critical $\tilde{\lambda}_c$ that satisfies Eq. (58) in our scheme is

$$\tilde{\lambda}_c = \sqrt{\frac{6}{4-d}} \sqrt{\frac{\zeta_m}{\varepsilon}}. \quad (70)$$

Given d , the first square root is a number; the second one is the result from step (ii) above.

It is interesting to see how the different exponents depend on $\tilde{\lambda}$, that is why we solve the flow equations for different $\tilde{\lambda}$ instead of plugging the value given by Eq. (58).

2. $d = 1$

The procedure and the values obtained for different $\tilde{\lambda}$ are shown for $d = 1$ in Fig. 8. We see that ζ_m/ε slightly decreases from its qEW value of $\zeta_m^{\text{qEW}} = 1/3$. The ratio ζ_m/ζ starts at 1 for $\tilde{\lambda} = 0$ and then grows. The effective force correlator becomes irrelevant for $\tilde{\lambda} \approx 1.4$. At the same time the bound (65) for \mathcal{A} (marked here as a red dashed line $\mathcal{A}/4 = 0.5$) is violated. The critical $\lambda_c = 0.755203$ respects all bounds in Eq. (69). It gives

$$\zeta_m^{d=1} = 0.8555, \quad (71)$$

$$\zeta^{d=1} = 0.6994, \quad (72)$$

$$z^{d=1} = 1.2736, \quad (73)$$

$$\mathcal{A}^{d=1} = 1.2781. \quad (74)$$

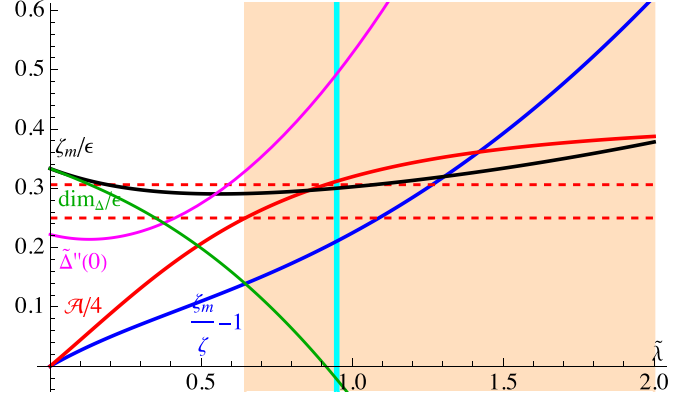


FIG. 9. Same as Fig. 8 for $d = 2$. The lower red dashed line is the bound on \mathcal{A} from $\mathcal{A}_c^{f_c}$, the upper one the bound from \mathcal{A}_c^Δ .

This can be compared to their values for $\lambda = 0$ (qEW), $\zeta_m = \zeta = 1$, and $z = 4/3$, and the numerically obtained values $\zeta_m = 1.052$, $\zeta = 0.636$, and $z = 1.1$. The values (71)–(73) are pretty reasonable for one-loop estimates: For qEW ζ in $d = 1$ comes out 20% smaller (1 instead of 1.25); the same reduction applies to our prediction for ζ_m in qKPZ. ζ is about 10% larger than the numerical value. Finally, while z is too large, using the numerically known value for ζ/ζ_m with the same one-loop estimate would yield $z = 0.942$, smaller than the measured value of $z = 1.1$. (Note that the prediction of $z = 1$ in [20] is invalidated by numerics [22].)

3. $d = 2$

Relevant quantities as a function of λ are given in Fig. 9. Evaluation at $\lambda = \lambda_c$ yields

$$\zeta_m^{d=2} = 0.6051, \quad (75)$$

$$\zeta^{d=2} = 0.4941, \quad (76)$$

$$z^{d=2} = 1.4112, \quad (77)$$

$$\mathcal{A}^{d=2} = 1.2479. \quad (78)$$

These results violate the bound (68) on \mathcal{A} for f_c . Supposing that this is an artifact of the one-loop approximation, the next bound to consider is the bound (65), asking that the effective force correlator is relevant at the transition. This bound is only slightly violated. We therefore hope that the values given in Eqs. (75)–(78) are usable.

Our own numerical simulations [22] give $\zeta_m = 0.70(3)$, $\zeta = 0.47(3)$ for TL92, and $\zeta_m = 0.61(2)$, $\zeta = 0.48(2)$ for anharmonic depinning. We expect the latter to be more reliable as there are less finite-size corrections. The agreement is then excellent.

For comparison we note that one-loop qEW gives $\zeta_m = \zeta = 2/3$, and $z = 1.5556$, while numerics gives $\zeta = \zeta_m = 0.753(2)$ and $z = 1.56(6)$.

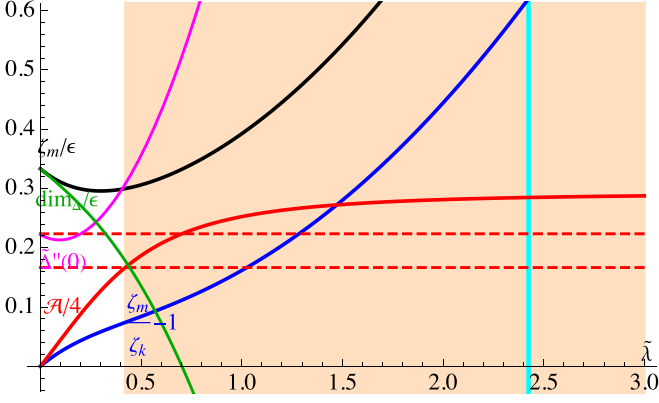


FIG. 10. Same as Fig. 8 for $d = 3$. The lower red dashed line is the bound on \mathcal{A} from \mathcal{A}_c^k , the upper one the bound from \mathcal{A}_c^Δ .

4. $d = 3$

Relevant quantities as a function of λ are given in Fig. 10. At the nontrivial fixed point (70) for λ , we find

$$\zeta_m^{d=3} \stackrel{?}{=} 0.9799, \quad (79)$$

$$\zeta^{d=3} \stackrel{?}{=} 0.6048, \quad (80)$$

$$z^{d=3} \stackrel{?}{=} 0.9777, \quad (81)$$

$$\mathcal{A}^{d=3} \stackrel{?}{=} 1.1394. \quad (82)$$

These values violate all bounds, and thus need to be rejected. There are four possible conclusions:

- (i) Since the effective force correlator is irrelevant at this fixed point, there is no qKPZ class.
- (ii) This fixed point is irrelevant, but there is a another fixed point not contained in our approach.
- (iii) Our approach is too crude.
- (iv) Our approach is crude as the fixed-point value for λ is too large, but providing a better value for λ_c it remains predictive.

If we believe Ref. [52], there is a distinguished fixed point for both classes, eliminating (i) while allowing for (ii). While the following option (iii) is suggestive, we can still try (iv): we use λ such that the effective depinning force at the fixed point is zero. Since the KPZ term grows under renormalization, it will finally render all pinned configurations unstable. This in turn reduces the generation of the KPZ term, making it less relevant. Our conjecture, which needs to be validated in numerical simulations, is that the system gets stuck at this precise point. Under this assumption we obtain

$$\zeta_m^{d=3} = 0.2998, \quad (83)$$

$$\zeta^{d=3} = 0.2751, \quad (84)$$

$$z^{d=3} = 1.7620, \quad (85)$$

$$\mathcal{A}^{d=3} = 0.6667. \quad (86)$$

These values are pretty much in line with the simulations for anharmonic depinning in $d = 3$: $\zeta_m = 0.34(3)$, $\zeta = 0.27(3)$. We do not know the values of z and \mathcal{A} .

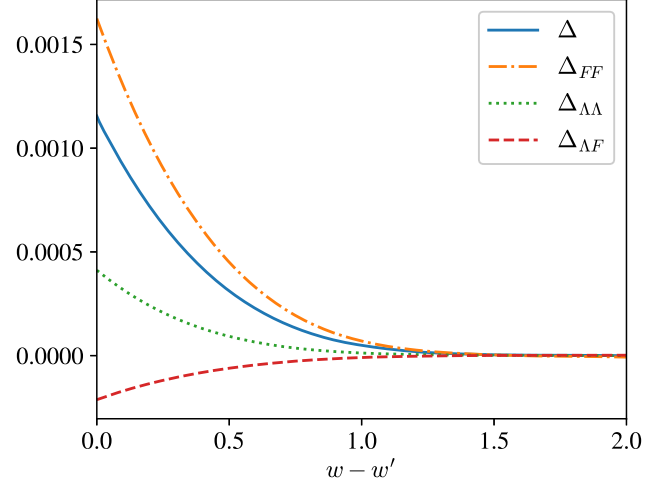


FIG. 11. Correlators of the disorder force, the interface center-of-mass, and the KPZ force, as well as the cross correlator of the KPZ force and the disorder force. The interface center-of-mass correlator is a mix of the disorder force and the KPZ force.

We remark that the behavior in $d = 3$ calls for more investigation: for example, d_c^{qKPZ} may be between 3 and 4.

5. Force amplitude ratio

Let us now address the relative fluctuations of forces defined in Eqs. (26) to (28). At leading order in perturbation theory we can estimate from Fig. 3 [where the $\delta_i \Delta(w)$ are defined] that

$$\frac{\Delta_{FF}(w)}{\Delta(w)} \approx \frac{\delta_1 \Delta(w)}{\delta_1 \Delta(w) + \delta_2 \Delta(w) + \delta_3 \Delta(w)}, \quad (87)$$

$$\frac{\Delta_{\Lambda\Lambda}(w)}{\Delta(w)} \approx \frac{\delta_2 \Delta(w)}{\delta_1 \Delta(w) + \delta_2 \Delta(w) + \delta_3 \Delta(w)}, \quad (88)$$

$$\frac{\Delta_{\Lambda F}(w)}{\Delta(w)} \approx \frac{\delta_3 \Delta(w)}{\delta_1 \Delta(w) + \delta_2 \Delta(w) + \delta_3 \Delta(w)}. \quad (89)$$

These equations simplify upon using that $\delta_3 \Delta(w) = 0$. Given the similar functional forms shown in Fig. 11, let us focus on the relative amplitudes. With the universal amplitude \mathcal{A} defined in Eq. (33), we get

$$\frac{\Delta_{FF}(0)}{\Delta(0)} \approx \frac{1}{1 - \frac{d(d+2)}{12} \mathcal{A}^2}, \quad (90)$$

$$\frac{\Delta_{\Lambda\Lambda}(0)}{\Delta(0)} \approx \frac{\frac{d(d+2)}{12} \mathcal{A}^2}{1 - \frac{d(d+2)}{12} \mathcal{A}^2}, \quad (91)$$

$$\frac{\Delta_{\Lambda F}(0)}{\Delta(0)} \approx 0. \quad (92)$$

In our simulations in $d = 1$ we find

$$\frac{\Delta_{FF}(0)}{\Delta(0)} = 1.40(3), \quad (93)$$

$$\frac{\Delta_{\Lambda\Lambda}(0)}{\Delta(0)} = 0.36(3), \quad (94)$$

$$\frac{\Delta_{\Lambda F}(0)}{\Delta(0)} = -0.18(3). \quad (95)$$

TABLE II. Correlator quantities coming from the analytical solution of the flow equations, setting $\tilde{\Delta}(0) = \varepsilon$. For qKPZ in $d = 3$ we fix $\tilde{\lambda}$ by supposing that the effective force correlator is marginal; the resulting values are indicated by an asterisk.

Quantity	d	qKPZ FT	qKPZ sim	qEW FT
κ	1	0.1291	0.12(1)	0.1667
	2	0.0738	0.07(1)	0.1667
	3	0.07704*	0.08(3)	0.1667

The theory in $d = 1$ has

$$\frac{d(d+2)}{12} \mathcal{A}^2 = 0.408, \quad (96)$$

which gives 1.69, 0.24, and 0 for the three ratios in Eqs. (93) to (95). Using the measured amplitude $\mathcal{A} = 1.1$ these ratios become 1.43, 0.21, and 0 which is closer to the measured amplitudes. All these values seem pretty reasonable given the order of approximation.

6. Other quantities and summary

Other properties of $\tilde{\Delta}(w)$ derived from the FRG solution are presented in Table II. An interesting property is the curvature κ , defined as

$$f(w) := \ln[\Delta(w)/\Delta(0)],$$

$$\kappa := \frac{1}{2} \frac{f''(0^+)}{f'(0^+)^2} = \frac{1}{2} \left[1 - \frac{\Delta(0)\Delta''(0^+)}{\Delta'(0^+)^2} \right]. \quad (97)$$

It is constructed such that an exponentially decaying $\Delta(w)$, which gives a straight line for $f(w)$, has a vanishing curvature. The definition was motivated by the observation in [34] that the FRG flow in the massless scheme possesses an exponentially decaying subspace, protected to all orders in perturbation theory. Our simulations in [22] showed no evidence for this subspace. Still, κ is a scale-free parameter which allows one to distinguish different shapes.

TABLE III. Critical exponents of the qKPZ class, from simulations of anharmonic depinning (except for z coming from TL92) and the analytical resolution of the fixed-point equations. In $d = 3$ we fix $\tilde{\lambda}$ by supposing that the depinning force remains positive, indicated by an asterisk. Note that our simulations agree with [52] and with the static exponents of [20] for $d \leq 2$; see [22] for a detailed discussion.

Exponent	Dimension (d)	Field theory	Simulations
ζ	1	0.6994	0.636(8)
	2	0.4941	0.48(2)
	3	0.2751*	0.27(3)
ζ_m	1	0.8555	1.052(5)
	2	0.6051	0.61(2)
	3	0.2998*	0.34(3)
z	1	1.2736	1.10(2)
	2	1.4112	
	3	1.762*	
\mathcal{A}	1	1.2781	1.1(1)
	2	1.2479	
	3	0.6667*	

Our results for the exponents are summarized in Table III and in Figs. 12 and 13 for the full function $\tilde{\Delta}(w)$, rescaled such that $\tilde{\Delta}(0) = -\tilde{\Delta}'(0^+) = 1$. They show excellent agreement between theory and simulation.

F. Cole-Hopf transformation

The Cole-Hopf transformation is defined by

$$Z(x, t) = e^{\hat{\lambda} u(x, t)} \Leftrightarrow u(x, t) = \frac{\ln Z(x, t)}{\hat{\lambda}}. \quad (98)$$

It is build to remove the nonlinear term proportional to λ from the KPZ equation (1) and reproduced here:

$$\eta \partial_t u(x, t) = c \nabla^2 u(x, t) + \lambda [\nabla u(x, t)]^2 + m^2 [w - u(x, t)] + F(x, u(x, t)). \quad (99)$$

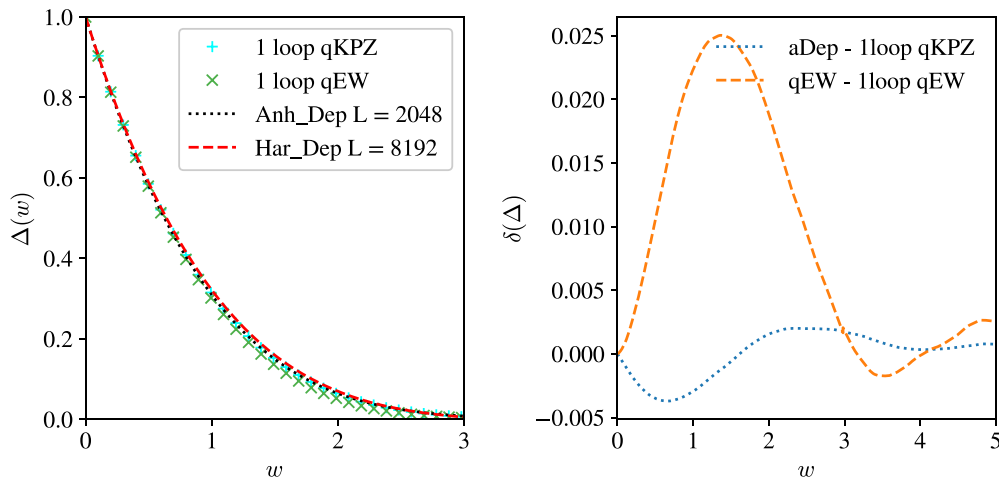


FIG. 12. (Left) Correlators in $d = 1$ from simulations of harmonic depinning (qEW) and anharmonic depinning (in the qKPZ universality class), compared to the analytic solution of the flow equations. $\Delta(w)$ for anharmonic depinning decays slightly faster than the one for harmonic depinning. The correlators are rescaled such that $\Delta(0) = |\Delta'(0^+)| = 1$. (Right) Difference of the rescaled correlators measured or analytical. The qKPZ FRG one-loop solution is around three times closer to the numerical simulation than the same curves for qEW.

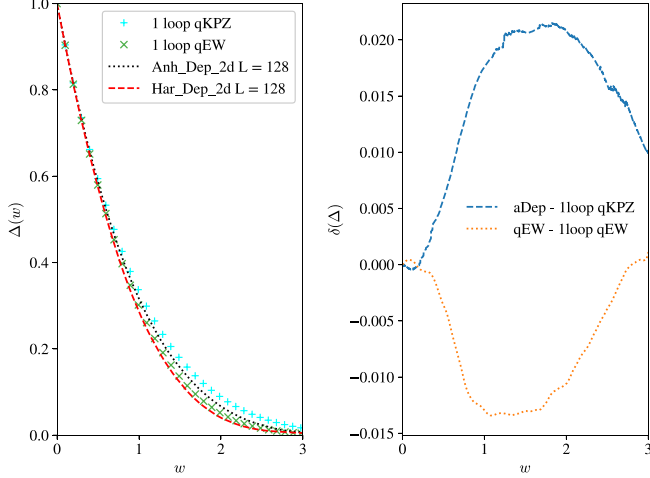


FIG. 13. (Left) Correlators in $d = 2$ from simulations of harmonic depinning (qEW) and anharmonic depinning (qKPZ class), compared to the solution of the FRG flow equations. The FRG solution is much closer to anharmonic depinning than to qEW. The correlators are rescaled such that $\Delta(0) = |\Delta'(0^+)| = 1$. (Right) Difference of the rescaled correlators measured and analytical. The agreement between simulations and theory is of the same order of magnitude for the two universality classes, even if the qKPZ theory is much more sophisticated.

The transformed equation reads

$$\eta \partial_t Z(x, t) = c \nabla^2 Z(x, t) + \hat{\lambda} Z(x, t) F\left(x, \frac{\ln Z(x, t)}{\hat{\lambda}}\right) + m^2 Z(x, t) [\hat{\lambda} w - \ln Z(x, t)]. \quad (100)$$

Some remarks are in order:

(i) While the term $\sim m^2$ in Eq. (99) provides a mass to the free propagator, i.e., a decay for large distances x proportional to $e^{-m|x|}$, it becomes a nonlinear term $\sim Z \ln Z$ in the transformed equation (100). For this reason one usually sets $m \rightarrow 0$.

(ii) The force $f = m^2 w$ in Eq. (99), which could be introduced independently of the term linear in $u(x, t)$, becomes a mass for the Cole-Hopf transformed theory (100), of the form $f \hat{\lambda} Z(x, t)$. As a result, the free propagator for Z decays with a factor of $e^{-|x| \sqrt{f \hat{\lambda}}}$.

This indicates that the Cole-Hopf transformation heavily shakes up infrared and ultraviolet properties of the theory. It may therefore not be surprising that in [34] no fixed point was found, whereas here, with properly defined physical fields, there is an FRG fixed point. A better understanding of the Cole-Hopf transformation and its consequences are desirable. We cannot exclude that it has some bearing on the perturbative treatment [53–56] of the KPZ equation itself, or on the mapping between the KPZ equation and the corresponding directed polymer problem [1,57], with all that this entails.

IV. PHYSICAL INSIGHTS

Let us summarize the main physical insights from our work:

(1) Most importantly, the qKPZ class covers a wide range of microscopic models and is universal. Strong evidence for this comes from the ability of the theory to predict not only the critical exponents, but also the effective KPZ amplitude \mathcal{A} , and the force correlator $\Delta(w)$.

(2) The introduction of the nonlinearity facilitates depinning as compared to qEW, Eq. (49). This favors “flatter” interfaces, i.e., those for which the integrated KPZ term is smaller, reducing the roughness exponent ζ .

(3) The renormalized force correlator in dimension $d = 1$ is close in shape to the correlator of qEW. This means that all properties linked to the shape of the correlator are close: for example, the avalanches-size correlations [58], or the correlation length ξ_\perp . The scaling dimension of ξ_\perp is close to its qEW counterpart, $\zeta_m^{\text{qKPZ}} \approx \zeta^{\text{qEW}}$, whereas the roughness exponents ζ are rather different.

(4) To properly renormalize the qKPZ class, one needs a confining potential. The confining potential forbids large fluctuations of the interface, which on the technical level provides a clear distinction between short-distance and long-distance divergences.

V. CONCLUSION

We revisited the qKPZ universality class. Using a careful comparison to numerical simulations in dimensions $d = 1$, $d = 2$, and $d = 3$, we constructed a consistent theory. The crucial ingredient is a flow equation for the KPZ nonlinearity, which is controlled by dimension d . Behind this feature lies the observation that all field theories for qEW with SR or LR elasticity, as well as qKPZ merge into a single theory in dimension $d = 0$. Our theory has predictive powers as long as we have a sufficient knowledge of the qEW fixed point in small dimensions and we are not too far away from $d = 0$. We derived several bounds, respected in low dimensions, but violated in dimension $d = 3$; there we currently can only close our scheme with an *ad hoc* assumption.

We hope that our method of first measuring the effective theory in a simulation, before attempting to build a field theory, can serve in other contexts as well. Applying our approach to other growth experiments for which no theory is available seems promising [59]. We hope it will also shed light on the problems in the standard (thermal) KPZ equation in higher dimensions.

ACKNOWLEDGMENTS

We thank Juan A. Bonachela and Miguel A. Muñoz for stimulating discussions and collaboration on the numerical part of this project, published in [22].

APPENDIX: FIELD-THEORY DETAILS

As explained in the main text, our field theory is massive, with a time-integrated response function given by $C_k = 1/(ck^2 + m^2)$. All diagrams are calculated with C_k . In this Appendix A 1 we first give all momentum integrals appearing in the main text or used later. In the following section, we recalculate all diagrams in the massive scheme.

1. Useful momentum integrals

To calculate all integrals, we use the Feynman representation of the time-integrated response,

$$C_k = \frac{1}{ck^2 + m^2} = \int_{s>0} e^{-s(cq^2 + m^2)}. \quad (\text{A1})$$

This lets appear a normalization factor

$$\int_k e^{-sk^2} = \frac{1}{(4\pi s)^{d/2}}. \quad (\text{A2})$$

The elasticity c and the mass m both appear in the momentum integrals, and can be taken out by a rescaling of k . As an example consider

$$\begin{aligned} I_1 &:= \int_k \frac{1}{(ck^2 + m^2)^2} = \frac{1}{c^{d/2}} \int_k \frac{1}{(k^2 + m^2)^2} \\ &= \frac{m^{d-4}}{c^{d/2}} \int_k \frac{1}{(k^2 + 1)^2} = \frac{m^{d-4}}{c^{d/2}} \int_k \int_{s>0} s e^{-s(k^2+1)} \\ &= \frac{m^{d-4}}{c^{d/2}} \frac{1}{(4\pi)^{d/2}} \int_{s>0} s^{1-d/2} = \frac{m^{d-4}}{c^{d/2}} \frac{2\Gamma(1+\frac{\varepsilon}{2})}{\varepsilon(4\pi)^{d/2}}. \end{aligned} \quad (\text{A3})$$

In the first step, we rescaled $k \rightarrow k\sqrt{c}$. In the second step $k \rightarrow \frac{k}{m}$. These steps assume that there are no explicit cutoffs on k , and that the only cutoff is set by m , and dimensional regularization is used. We then used the auxiliary integral (A1), and the momentum integral (A2). Below we give a complete list of all encountered integrals, after rescaling to eliminate the c and m dependence:

$$\int_k \frac{1}{k^2 + 1} = \frac{\Gamma(1 - \frac{d}{2})}{(4\pi)^{d/2}}, \quad (\text{A4})$$

$$\int_k \frac{k^2}{(k^2 + 1)^2} = \frac{d}{2} \int_k \frac{1}{k^2 + 1}, \quad (\text{A5})$$

$$\int_k \frac{1}{(k^2 + 1)^2} = \frac{\Gamma(2 - \frac{d}{2})}{(4\pi)^{d/2}} \equiv \frac{2\Gamma(1 + \frac{\varepsilon}{2})}{\varepsilon(4\pi)^{d/2}}, \quad (\text{A6})$$

$$\int_k \frac{k_1^2}{(k^2 + 1)^3} \equiv \frac{1}{4} \int_k \frac{1}{(k^2 + 1)^2}, \quad (\text{A7})$$

$$\int_k \frac{k^2}{(k^2 + 1)^3} \equiv \frac{d}{4} \int_k \frac{1}{(k^2 + 1)^2}, \quad (\text{A8})$$

$$\int_k \frac{k^4}{(k^2 + 1)^4} \equiv \frac{d(d+2)}{24} \int_k \frac{1}{(k^2 + 1)^2}. \quad (\text{A9})$$

Integral (A6) is the key integral used to define the renormalized force correlator $\hat{\Delta}(u)$; see Eqs. (54)–(51). It is therefore useful to express as far as possible all integrals w.r.t. to integral (A6), or including the dimensions w.r.t. integral (A3).

2. Diagrams

a. The coefficient a_0

According to Eq. (A3) in [34]

$$\text{Diagram} = \lambda \Delta'(0^+) \tilde{u} \dot{u} \int_k \frac{ck^2}{(ck^2 + m^2)^3}, \quad (\text{A10})$$

$$\begin{aligned} \int_k \frac{ck^2}{(ck^2 + m^2)^3} &= c^{-\frac{d}{2}} \int_k \frac{k^2}{(k^2 + m^2)^3} \\ &= c^{-\frac{d}{2}} m^{d-4} \int_k \frac{k^2}{(k^2 + 1)^3}. \end{aligned} \quad (\text{A11})$$

The relevant integral is Eq. (A8), thus in Eq. (40)

$$a_0 = \frac{d}{4}. \quad (\text{A12})$$

Note that it does not modify η in dimension $d = 0$.

b. The coefficient a_1

The first correction (in momentum space) to $\tilde{u} \nabla^2 u$ is

$$\begin{aligned} \text{Diagram} &= -2\Delta'(0^+) \lambda \int_k \frac{kp}{(c(k+p)^2 + m^2)(ck^2 + m^2)} \\ &= 4\Delta'(0^+) \lambda \int_k \frac{c(kp)^2}{(ck^2 + m^2)^3} + \mathcal{O}(p^3) \\ &= \Delta'(0^+) \hat{\lambda}(cp^2) I_1. \end{aligned} \quad (\text{A13})$$

Note that $-p^2 u \leftrightarrow \nabla^2 u$. This yields in Eq. (41)

$$a_1 = 1. \quad (\text{A14})$$

c. The coefficient a_2

The second correction (in momentum space) to $\tilde{u} \nabla^2 u$ is

$$\begin{aligned} \text{Diagram} &= -4\Delta(0) \lambda^2 \int_k \frac{(kp)[k(k+p)]}{(c(k+p)^2 + m^2)(ck^2 + m^2)^2} \\ &= \frac{4\Delta(0) \lambda^2}{c^{d/2+1}} \int_k \frac{2k^2(kp)^2}{(k^2 + m^2)^4} - \frac{(kp)^2}{(k^2 + m^2)^3} + \mathcal{O}(p^3) \\ &= 4\Delta(0) \hat{\lambda}^2 (cp^2) I_1 \frac{d-1}{3}. \end{aligned} \quad (\text{A15})$$

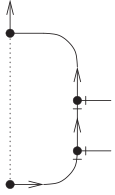
This implies in Eq. (41)

$$a_2 = \frac{d-1}{3}. \quad (\text{A16})$$

d. The coefficient a_3

Denoting by p_1 and p_2 the momenta entering into the two external fields to the right, we have up to higher-order

corrections in the p_i



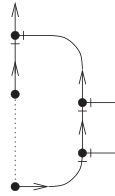
$$\begin{aligned}
 &= \int_k 4\lambda^2 \Delta'(0^+) \frac{(kp_1)^\alpha (kp_2)^\beta}{(ck^2 + m^2)^3} \tilde{u}_{-p_1-p_2} u_{p_1} u_{p_2} \\
 &= \int_k 4\lambda^2 \Delta'(0^+) \frac{\frac{k^2}{d} (p_1 \cdot p_2)}{(ck^2 + m^2)^3} \tilde{u}_{-p_1-p_2} u_{p_1} u_{p_2} \\
 &= - \int_k 4\lambda^2 \Delta'(0^+) \frac{\frac{k^2}{d}}{(ck^2 + m^2)^3} \tilde{u}(\nabla u)^2 \\
 &= -4\Delta'(0^+) \frac{\lambda^2}{d} \int_k \frac{k^2}{(ck^2 + m^2)^3} \tilde{u}(\nabla u)^2 \\
 &= -\Delta'(0^+) \lambda \hat{I}_1 \tilde{u}(\nabla u)^2. \tag{A17}
 \end{aligned}$$

We used Eq. (A9). This yields in Eq. (42)

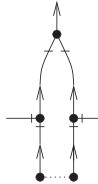
$$a_3 = 1. \tag{A18}$$

e. The coefficient a_4

In this appendix we list and evaluate all diagrams encountered in the main text.



$$= -8 \frac{\Delta(0)}{d} \lambda^3 \int_k \frac{k^4}{(ck^2 + m^2)^4} \tilde{u}(\nabla u)^2, \tag{A19}$$



$$= 4 \frac{\Delta(0)}{d} \lambda^3 \int_k \frac{k^4}{(ck^2 + m^2)^4} \tilde{u}(\nabla u)^2. \tag{A20}$$

Together their amplitude [without the factor of $\Delta(0)$ and $\tilde{u}(\nabla u)^2$] is

$$-\frac{4\lambda^3}{dc^{d/2+2}} \int \frac{k^4}{(k^2 + m^2)^4} = -\lambda \hat{\lambda}^2 \frac{d+2}{6} I_1. \tag{A21}$$

Therefore in Eq. (42),

$$a_4 = \frac{d+2}{6}. \tag{A22}$$

f. The coefficient a_5

It is given by twice the integral (A9); thus for Eq. (43),

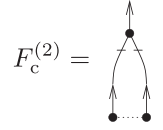
$$a_5 = \frac{d(d+2)}{12}. \tag{A23}$$

3. Depinning force

The perturbative calculation gives in absence of KPZ terms

$$F_c^{(1)} = -\Delta'(0^+) \int_k \frac{1}{ck^2 + m^2}. \tag{A24}$$

The contribution induced by the KPZ term is



$$F_c^{(2)} = \lambda \Delta(0) \int_k \frac{k^2}{(ck^2 + m^2)^2}. \tag{A25}$$

[There is a combinatorial factor of 1/2 from $\Delta(u_t - u_t)$, followed by a 2 for the number of possible contractions.] The total is

$$\begin{aligned}
 F_c &= F_c^{(1)} + F_c^{(2)} \\
 &\simeq \left[\Delta'(0^+) + \frac{d}{2} \frac{\lambda}{c} \Delta(0) \right] \int_k \frac{1}{ck^2 + m^2}. \tag{A26}
 \end{aligned}$$

- [1] K. J. Wiese, Theory and experiments for disordered elastic manifolds, depinning, avalanches, and sandpiles, *Rep. Prog. Phys.* **85**, 086502 (2022).
- [2] L.-H. Tang, M. Kardar, and D. Dhar, Driven Depinning in Anisotropic Media, *Phys. Rev. Lett.* **74**, 920 (1995).
- [3] H. Barkhausen, Zwei mit Hilfe der neuen Verstärker entdeckte Erscheinungen, *Phys. Z.* **20**, 401 (1919).
- [4] G. Durin and S. Zapperi, *The Barkhausen effect*, in *The Science of Hysteresis*, edited by G. Bertotti and I. Mayergoyz (Academic Press, Amsterdam, 2006), Vol. II, pp. 181–267.
- [5] G. Durin, F. Bohn, M. A. Correa, R. L. Sommer, P. Le Doussal, and K. J. Wiese, Quantitative Scaling of Magnetic Avalanches, *Phys. Rev. Lett.* **117**, 087201 (2016).
- [6] C. ter Burg, F. Bohn, F. Durin, R. L. Sommer, and K. J. Wiese, Force Correlations in Disordered Magnets, *Phys. Rev. Lett.* **129**, 107205 (2022).
- [7] S. Scheidl and V. M. Vinokur, Driven dynamics of periodic elastic media in disorder, *Phys. Rev. E* **57**, 2574 (1998).
- [8] H. Bucheli, O. S. Wagner, V. B. Geshkenbein, A. I. Larkin, and G. Blatter, $(4+N)$ -dimensional elastic manifolds in random media: A renormalization-group analysis, *Phys. Rev. B* **57**, 7642 (1998).
- [9] O. Narayan and D. S. Fisher, Critical behavior of sliding charge-density waves in $4-\epsilon$ dimensions, *Phys. Rev. B* **46**, 11520 (1992).
- [10] K. J. Wiese, M. Bercy, L. Melkonyan, and T. Bizebard, Universal force correlations in an RNA-DNA unzipping experiment, *Phys. Rev. Res.* **2**, 043385 (2020).
- [11] P. Le Doussal, K. J. Wiese, E. Raphael, and R. Golestanian, Can Nonlinear Elasticity Explain Contact-Line Roughness at Depinning? *Phys. Rev. Lett.* **96**, 015702 (2006).
- [12] C. Bachas, P. Le Doussal, and K. J. Wiese, Wetting and minimal surfaces, *Phys. Rev. E* **75**, 031601 (2007).
- [13] P. Le Doussal, K. J. Wiese, S. Moulinet, and E. Rolley, Height fluctuations of a contact line: A direct measurement of the renormalized disorder correlator, *Europhys. Lett.* **87**, 56001 (2009).

- [14] D. S. Fisher, Collective transport in random media: From superconductors to earthquakes, *Phys. Rep.* **301**, 113 (1998).
- [15] D. S. Fisher, K. Dahmen, S. Ramanathan, and Y. Ben-Zion, Statistics of Earthquakes in Simple Models of Heterogeneous Faults, *Phys. Rev. Lett.* **78**, 4885 (1997).
- [16] S. Poincloux, M. Adda-Bedia, and F. Lechenault, Geometry and Elasticity of a Knitted Fabric, *Phys. Rev. X* **8**, 021075 (2018).
- [17] S. Poincloux, M. Adda-Bedia, and F. Lechenault, Crackling Dynamics in the Mechanical Response of Knitted Fabrics, *Phys. Rev. Lett.* **121**, 058002 (2018).
- [18] S. V. Buldyrev, A.-L. Barabási, F. Caserta, S. Havlin, H. E. Stanley, and T. Vicsek, Anomalous interface roughening in porous media: Experiment and model, *Phys. Rev. A* **45**, R8313 (1992).
- [19] L.-H. Tang and H. Leschhorn, Pinning by directed percolation, *Phys. Rev. A* **45**, R8309 (1992).
- [20] L. A. N. Amaral, A.-L. Barabási, S. V. Buldyrev, S. T. Harrington, S. Havlin, R. Sadr-Lahijany, and H. E. Stanley, Avalanches and the directed percolation depinning model: Experiments, simulations, and theory, *Phys. Rev. E* **51**, 4655 (1995).
- [21] A. Rosso and W. Krauth, Origin of the Roughness Exponent in Elastic Strings at the Depinning Threshold, *Phys. Rev. Lett.* **87**, 187002 (2001).
- [22] G. Mukerjee, J. A. Bonachela, M. A. Muñoz, and K. J. Wiese, Depinning in the quenched Kardar-Parisi-Zhang class. I. Mappings, simulations, and algorithm, *Phys. Rev. E* **107**, 054136 (2023).
- [23] K.-W. Moon, D.-H. Kim, S.-C. Yoo, C.-G. Cho, S. Hwang, B. Kahng, B.-C. Min, K.-H. Shin, and S.-B. Choe, Distinct Universality Classes of Domain Wall Roughness in Two-Dimensional Pt/Co/Pt Films, *Phys. Rev. Lett.* **110**, 107203 (2013).
- [24] R. Díaz Pardo, N. Moisan, L. J. Albornoz, A. Lemaître, J. Curiale, and V. Jeudy, Common universal behavior of magnetic domain walls driven by spin-polarized electrical current and magnetic field, *Phys. Rev. B* **100**, 184420 (2019).
- [25] M. A. C. Huergo, N. E. Muzzio, M. A. Pasquale, P. H. Pedro González, A. E. Bolzán, and A. J. Arvia, Dynamic scaling analysis of two-dimensional cell colony fronts in a gel medium: A biological system approaching a quenched Kardar-Parisi-Zhang universality, *Phys. Rev. E* **90**, 022706 (2014).
- [26] S. Atis, A. K. Dubey, D. Salin, L. Talon, P. Le Doussal, and K. J. Wiese, Experimental Evidence for Three Universality Classes for Reaction Fronts in Disordered Flows, *Phys. Rev. Lett.* **114**, 234502 (2015).
- [27] O. Narayan and D. S. Fisher, Dynamics of Sliding Charge-Density Waves in $4-\epsilon$ Dimensions, *Phys. Rev. Lett.* **68**, 3615 (1992).
- [28] O. Narayan and D. S. Fisher, Threshold critical dynamics of driven interfaces in random media, *Phys. Rev. B* **48**, 7030 (1993).
- [29] H. Leschhorn, T. Nattermann, S. Stepanow, and L.-H. Tang, Driven interface depinning in a disordered medium, *Ann. Phys.* **509**, 1 (1997).
- [30] T. Nattermann, S. Stepanow, L.-H. Tang, and H. Leschhorn, Dynamics of interface depinning in a disordered medium, *J. Phys. II France* **2**, 1483 (1992).
- [31] P. Chauve, P. Le Doussal, and K. J. Wiese, Renormalization of Pinned Elastic Systems: How Does It Work beyond One Loop? *Phys. Rev. Lett.* **86**, 1785 (2001).
- [32] P. Le Doussal, K. J. Wiese, and P. Chauve, Two-loop functional renormalization group analysis of the depinning transition, *Phys. Rev. B* **66**, 174201 (2002).
- [33] P. Le Doussal, K. J. Wiese, and P. Chauve, Functional renormalization group and the field theory of disordered elastic systems, *Phys. Rev. E* **69**, 026112 (2004).
- [34] P. Le Doussal and K. J. Wiese, Functional renormalization group for anisotropic depinning and relation to branching processes, *Phys. Rev. E* **67**, 016121 (2003).
- [35] P. Le Doussal and K. J. Wiese, Driven particle in a random landscape: Disorder correlator, avalanche distribution and extreme value statistics of records, *Phys. Rev. E* **79**, 051105 (2009).
- [36] P. Grassberger, D. Dhar, and P. K. Mohanty, Oslo model, hyperuniformity, and the quenched Edwards-Wilkinson model, *Phys. Rev. E* **94**, 042314 (2016).
- [37] A. Shapira and K. J. Wiese, Anchored advected interfaces, Oslo model, and roughness at depinning, *arXiv:2302.13749* [J. Stat. Mech. (to be published)].
- [38] P. C. Martin, E. D. Siggia, and H. A. Rose, Statistical dynamics of classical systems, *Phys. Rev. A* **8**, 423 (1973).
- [39] P. Le Doussal and K. J. Wiese, How to measure functional RG fixed-point functions for dynamics and at depinning, *Europhys. Lett.* **77**, 66001 (2007).
- [40] A. A. Middleton, P. Le Doussal, and K. J. Wiese, Measuring Functional Renormalization Group Fixed-Point Functions for Pinned Manifolds, *Phys. Rev. Lett.* **98**, 155701 (2007).
- [41] A. Rosso, P. Le Doussal, and K. J. Wiese, Numerical calculation of the functional renormalization group fixed-point functions at the depinning transition, *Phys. Rev. B* **75**, 220201(R) (2007).
- [42] J. A. Bonachela, M. Alava, and M. A. Muñoz, Cusps in systems with (many) absorbing states, *Phys. Rev. E* **79**, 050106 (2009).
- [43] A.-L. Barabási, G. Grinstein, and M. A. Muñoz, Directed Surfaces in Disordered Media, *Phys. Rev. Lett.* **76**, 1481 (1996).
- [44] H. Hinrichsen, Non-equilibrium critical phenomena and phase transitions into absorbing states, *Adv. Phys.* **49**, 815 (2000).
- [45] N. Araújo, P. Grassberger, B. Kahng, K. J. Schrenk, and R. M. Ziff, Recent advances and open challenges in percolation, *Eur. Phys. J. Spec. Top.* **223**, 2307 (2014).
- [46] D. Dhar, Directed percolation and directed animals, *arXiv:1703.07541*.
- [47] G. Parisi, *Statistical Field Theory*, Frontiers in Physics (Addison-Wesley, New York, 1988).
- [48] G. Parisi, Field-theoretic approach to second-order phase transitions in two- and three-dimensional systems, *J. Stat. Phys.* **23**, 49 (1980).
- [49] G. A. Baker, B. G. Nickel, M. S. Green, and D. I. Meiron, Ising-Model Critical Indices in Three Dimensions from the Callan-Symanzik Equation, *Phys. Rev. Lett.* **36**, 1351 (1976).
- [50] B. G. Nickel, D. I. Meiron, and G. A. Baker, Compilation of 2-pt and 4-pt graphs for continuous spin models, University of Guelph report, 1977 (unpublished).
- [51] G. A. Baker, B. G. Nickel, and D. I. Meiron, Critical indices from perturbation analysis of the Callan-Symanzik equation, *Phys. Rev. B* **17**, 1365 (1978).
- [52] A. Rosso, A. K. Hartmann, and W. Krauth, Depinning of elastic manifolds, *Phys. Rev. E* **67**, 021602 (2003).

- [53] E. Frey and U. C. Täuber, Two-loop renormalization group analysis of the Burgers-Kardar-Parisi-Zhang equation, *Phys. Rev. E* **50**, 1024 (1994).
- [54] M. Lässig, On the renormalization of the Kardar-Parisi-Zhang equation, *Nucl. Phys. B* **448**, 559 (1995).
- [55] K. J. Wiese, Critical discussion of the two-loop calculations for the KPZ-equation, *Phys. Rev. E* **56**, 5013 (1997).
- [56] K. J. Wiese, On the perturbation expansion of the KPZ-equation, *J. Stat. Phys.* **93**, 143 (1998).
- [57] P. Le Doussal and K. J. Wiese, Two-loop functional renormalization for elastic manifolds pinned by disorder in N dimensions, *Phys. Rev. E* **72**, 035101(R) (2005).
- [58] T. Thiery, P. Le Doussal, and K. J. Wiese, Universal correlations between shocks in the ground state of elastic interfaces in disordered media, *Phys. Rev. E* **94**, 012110 (2016).
- [59] C. S. Dias, P. J. Yunker, A. G. Yodh, N. A. M. Araújo, and M. M. Telo da Gama, Interaction anisotropy and the KPZ to KPZQ transition in particle deposition at the edges of drying drops, *Soft Matter* **14**, 1903 (2018).